

Activation of Methane by Oligomeric $(\text{Al}_2\text{O}_3)_x^+$ ($x = 3, 4, 5$): The Role of Oxygen-Centered Radicals in Thermal Hydrogen-Atom Abstraction**

Sandra Feyel, Jens Döbler, Robert Höckendorf, Martin K. Beyer, Joachim Sauer,* and Helmut Schwarz*

Dedicated to Professor Charles DePuy on the occasion of his 80th birthday

Selective activation of C–H bonds constitutes a major challenge in the syntheses of added-value products. For methane in particular, a number of factors make the activation difficult: CH_4 is thermodynamically the most stable of all alkanes ($\Delta_f G^0 = -50.8 \text{ kJ mol}^{-1}$),^[1] and the C–H bond strength is the largest of all sp^3 -hybridized hydrocarbons (439 kJ mol^{-1}).^[2] Furthermore, the negative electron affinity, a large ionization energy, the wide HOMO/LUMO gap, an extremely high $\text{p}K_a$ value, and its relatively modest proton affinity are very unfavorable intrinsic factors for its activation.^[3,4]

Hydrogen atom abstraction from CH_4 to generate CH_3 is viewed as a decisive step in the oxidative dehydrogenation and dimerization of methane [Equation (1)]. Various metal oxides MO have proven useful to induce the initial homolytic C–H bond cleavage,^[5] which typically requires rather elevated temperatures.



As demonstrated previously, several simple cationic metal oxides are also capable of bringing about thermal activation of methane in the gas phase according to Equation (1a), and typical examples include: FeO^+ ,^[6] MoO_3^+ ,^[7] $\text{ReO}_3(\text{OH})^+$,^[8] OsO_4^+ ,^[9] and $\text{V}_4\text{O}_{10}^+$.^[10] Interestingly, not only these transition-metal based oxides but also the main-group metal oxide

MgO^+ exhibits this reactivity.^[11] $\text{V}_4\text{O}_{10}^+$ has been so far the only polynuclear oxide species for which thermal activation of methane has been observed.^[10] Herein we show that also main-group metal polynuclear oxide cations are capable of inducing hydrogen-atom abstraction from methane, and some principal aspects about the roles of spin and thermochemistry underlying this elementary process will be discussed.

Computational analysis of the above-mentioned metal oxide radical cations reveals that they all have a high spin density at an oxygen atom in common; thus, an $[\text{O}-\text{M}]^+$ unit is formed upon electron removal from the metal–oxo bond of the corresponding neutral species.^[12–14] It is our conjecture that the doublet character of these ions makes them reactive toward thermal hydrogen-atom abstraction, provided the resulting H–O bond is stronger than the C–H bond that is to be broken homolytically (Table 1).^[15] As reported earlier,^[16]

Table 1: Reaction enthalpies ($-\Delta_r H_0$) for the reaction $\frac{1}{2}\text{H}_2 + [\text{O}-\text{M}]^+ \rightarrow [\text{HO}-\text{M}]^+$.^[a]

Reactive cations $[\text{O}-\text{M}]^+$	$\Delta_r H_0$ [kJ mol ⁻¹]
MgO^+	292 ^[b]
FeO^+	244 ^[b] (210–220) ^[c]
MoO_3^+	290 ^[b]
$\text{ReO}_3(\text{OH})^+$	290 ^[b]
OsO_4^+	284 ^[b]
$\text{V}_4\text{O}_{10}^+$	294 ^[b]
$\text{Al}_8\text{O}_{12}^+$	298 ^[b]

[a] For the reference reaction $\text{CH}_4 \rightarrow \text{CH}_3 + \frac{1}{2}\text{H}_2$, $\Delta_r H_0$ amounts to 207 kJ mol^{-1} (B3LYP/TZVP).^[17] [b] Calculations performed using B3LYP/TZVP. [c] CASPT2.

the open-shell cluster $\text{Al}_8\text{O}_{12}^+$ exhibits the aforementioned structural, electronic and energetic features with a high spin density on the terminal oxygen atom (Figure 1).

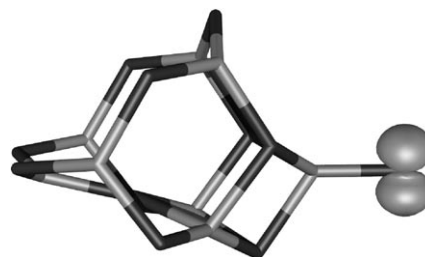


Figure 1. Spin density for the optimized structure of $\text{Al}_8\text{O}_{12}^+$. Dark vertices O, light vertices Al.

[*] Dr. J. Döbler, Prof. Dr. J. Sauer
Institut für Chemie, Technische Universität Berlin
Straße des 17. Juni 135, 10623 Berlin (Germany)
Fax: (+49) 30-314-21102
E-mail: js@chemie.hu-berlin.de

Dipl.-Chem. S. Feyel, Dipl.-Chem. R. Höckendorf,^[†]
Prof. Dr. M. K. Beyer,^[†] Prof. Dr. H. Schwarz
Institut für Chemie, Humboldt-Universität Berlin
Unter den Linden 6, 10099 Berlin (Germany)
Fax: (+49) 30-2093-7136
E-mail: helmut.schwarz@mail.chem.tu-berlin.de

[†] New Address: Institut für Physikalische Chemie, Christian-Albrechts-Universität zu Kiel, Olshausenstraße 40, 24098 Kiel (Germany)

[**] Support by the Fonds der Chemischen Industrie and the Deutsche Forschungsgemeinschaft (Cluster of Excellence “Unifying Concepts in Catalysis”) is acknowledged. We appreciate helpful discussions with and comments by Dr. Detlef Schröder.

Supporting information for this article is available on the WWW under <http://www.angewandte.org> or from the author.

With these predictions in mind, we set out to study experimentally the $\text{Al}_8\text{O}_{12}^{+}/\text{CH}_4$ system. The experiments were performed with a FT-ICR mass spectrometer equipped with an external laser vaporization source. The latter is used to generate a broad distribution of aluminum oxide cations of the general formula $\text{Al}_n\text{O}_m^{+}$ ($n=6-10$, $m=8-15$), which after mass selection are reacted with methane. $\text{Al}_8\text{O}_{12}^{+}$ brings about the abstraction of a hydrogen atom from methane (Figure 2a) with an absolute rate constant of $k_{\text{abs}}=3.8 \times$

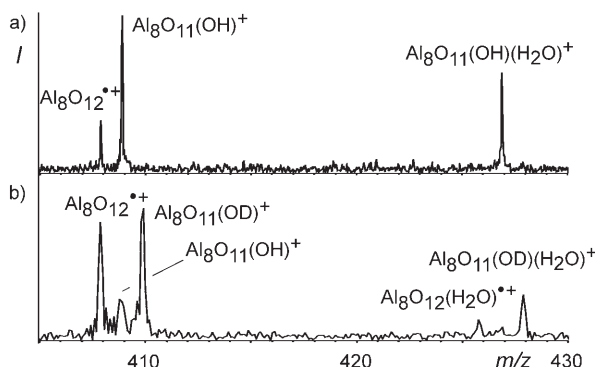


Figure 2. IMR of mass-selected $\text{Al}_8\text{O}_{12}^{+}$ with a) CH_4 with a reaction delay of 35 s and b) CD_4 with a reaction delay of 40 s at stationary pressures of 9×10^{-8} mbar.^[18]

$10^{-12} \text{ cm}^3 \text{ molecule}^{-1} \text{ s}^{-1}$ (Table 2). Likewise, labeling experiments using CD_4 (Figures 2b and 3) demonstrate methane activation by $\text{Al}_8\text{O}_{12}^{+}$ to yield $\text{Al}_8\text{O}_{11}(\text{OD})^{+}$. However, from inspection of Figures 2b and 3, it is clear that the ion/molecule

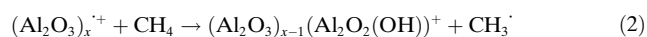
Table 2: Upper limits for KIEs and absolute rate constants for the reactions $(\text{Al}_2\text{O}_3)_x^{+} + \text{CD}_4 \rightarrow (\text{Al}_2\text{O}_3)_{x-1}(\text{Al}_2\text{O}_2(\text{OD}))^{+} + \text{CD}_3^{\cdot}$ ($x=3, 4$).

x	KIE	$k_{\text{abs}} [10^{-12} \text{ cm}^3 \text{ molecule}^{-1} \text{ s}^{-1}]^{\text{a}}$
3	< 2.5	1.8
4	< 2.4 ± 0.5	3.8

[a] The error bars are estimated to be $\pm 30\%$.

reaction (IMR) of $\text{Al}_8\text{O}_{12}^{+}$ with CD_4 also resulted in a mass gain of ($\Delta m = +1$). As this feature cannot derive from the IMR with CD_4 , we assume that the aluminum oxide cation abstracts a hydrogen atom from any remaining organic substrate in the cell, as for instance from residual oil vapor or from other reactants used before to produce the light aluminum hydroxide $\text{Al}_8\text{O}_{11}(\text{OH})^{+}$ (Figure 2).^[18]

Perhaps not surprisingly, it turns out that all of the investigated oligomeric species of $(\text{Al}_2\text{O}_3)_x^{+}$ with $x=3, 4$, and 5, (namely $\text{Al}_6\text{O}_9^{+}$, $\text{Al}_8\text{O}_{12}^{+}$, and $\text{Al}_{10}\text{O}_{15}^{+}$) react spontaneously with methane according to Equation (2) ($x=3, 4$, and 5).



IMR of $\text{Al}_6\text{O}_9^{+}$ with CD_4 also resulted in two signals at $\Delta m = +1$ and $\Delta m = +2$, which are assigned to $\text{Al}_6\text{O}_8(\text{OH})^{+}$ and $\text{Al}_6\text{O}_8(\text{OD})^{+}$ ($k_{\text{abs}} = 1.8 \times 10^{-12} \text{ cm}^3 \text{ molecule}^{-1} \text{ s}^{-1}$;

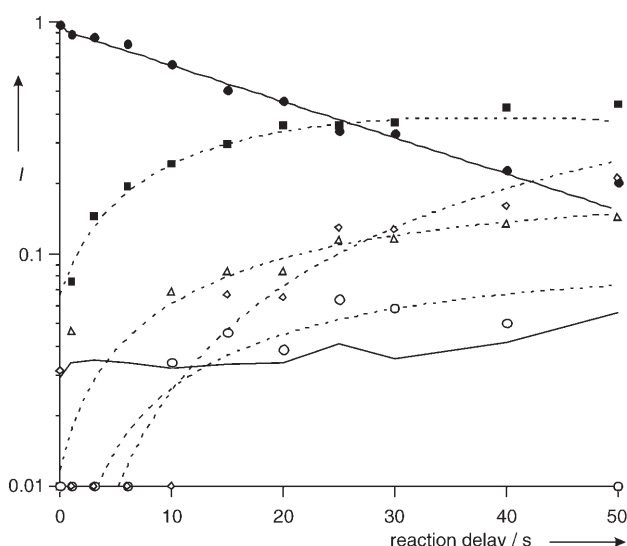


Figure 3. Temporal intensity profile for the reaction of mass-selected $\text{Al}_8\text{O}_{12}^{+}$ with CD_4 ; $p(\text{CD}_4) = 9 \times 10^{-8}$ mbar. ●: $\text{Al}_8\text{O}_{12}^{+}$; △: $\text{Al}_8\text{O}_{11}(\text{OH})^{+}$; ■: $\text{Al}_8\text{O}_{11}(\text{OD})^{+}$; ○: $\text{Al}_8\text{O}_{12}(\text{H}_2\text{O})^{+}$; ◇: $\text{Al}_8\text{O}_{11}(\text{OD})(\text{H}_2\text{O})^{+}$. Gray line denotes noise level.

Table 2), respectively. Although the IMR with background gases prevents an accurate determination of the kinetic isotope effects (KIEs), upper limits can nevertheless be estimated (Table 2).

From the occurrence of reaction (2) it follows that the bond energy of the newly formed O–H bond in all three ionic clusters, $(\text{Al}_6\text{O}_8)(\text{OH})^{+}$, $(\text{Al}_8\text{O}_{11})(\text{OH})^{+}$, and $(\text{Al}_{10}\text{O}_{14})(\text{OH})^{+}$ must exceed the C–H bond energy of methane, that is, 439 kJ mol^{-1} .^[2]

Although adduct formations like $(\text{Al}_2\text{O}_3)_x(\text{CH}_4)^{+}$ and $(\text{Al}_2\text{O}_3)_x(\text{CD}_4)^{+}$ have not been observed, complexes with background water were generated in the reactions with both CH_4 and CD_4 as primary as well as secondary reaction products, such as $(\text{Al}_2\text{O}_3)_x(\text{H}_2\text{O})^{+}$, $(\text{Al}_2\text{O}_3)_{x-1}(\text{Al}_2\text{O}_2(\text{OH})(\text{H}_2\text{O}))^{+}$, and $(\text{Al}_2\text{O}_3)_{x-1}(\text{Al}_2\text{O}_2(\text{OD})(\text{H}_2\text{O}))^{+}$ (Figure 2).

Not unexpectedly, the reactions of aluminum oxide cluster cations with an odd number of aluminum atoms, such as $\text{Al}_7\text{O}_9^{+}$, $\text{Al}_7\text{O}_{10}^{+}$, $\text{Al}_7\text{O}_{11}^{+}$, $\text{Al}_9\text{O}_{13}^{+}$, and $\text{Al}_9\text{O}_{14}^{+}$, with methane reveal that none of these clusters resulted in any bond activation of the hydrocarbon. As these oxides are lacking the obviously crucial presence of an oxygen-centered radical, their nonreactivity underlines the validity of our generalized concept of hydrogen-atom abstraction from methane by metal oxides.^[15]

As to the mechanistic details, a closer computational inspection of the potential energy surface (PES) for the $\text{Al}_8\text{O}_{12}^{+}/\text{CH}_4$ system by DFT calculations reveals some subtle differences when compared with the $\text{V}_4\text{O}_{10}^{+}/\text{CH}_4$ case: For the latter it was found^[10] that the reaction proceeds by a barrierless direct hydrogen abstraction, with no encounter complex of the type $\text{V}_4\text{O}_{10}^{+}\text{CH}_4$ being located on the PES. In contrast, for the $\text{Al}_8\text{O}_{12}^{+}/\text{CH}_4$ system a minimum structure corresponding to an encounter complex exists (Figures 4 and 5a), in which one hydrogen atom interacts with the radical center of the oxygen atom ($\Delta_r H_0 = -10 \text{ kJ mol}^{-1}$). The

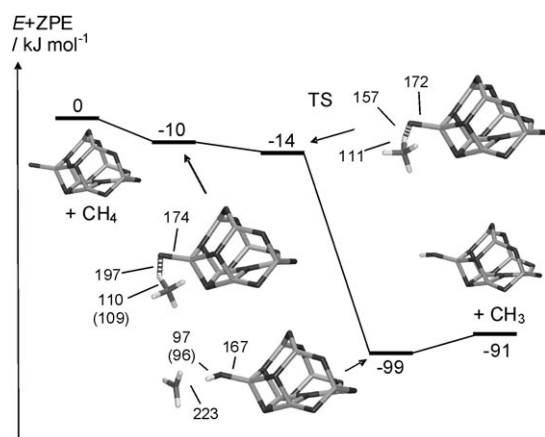


Figure 4. Energy diagram for the reaction of $\text{Al}_8\text{O}_{12}^{+}$ with methane. The values are relative to the entrance channel, corrected for zero-point energy (ZPE) and given in kJ mol^{-1} . For the stationary points of the reaction, the C–H, H–O, and O–Al distances are given in pm (with distances of the unperturbed fragments in parentheses.)

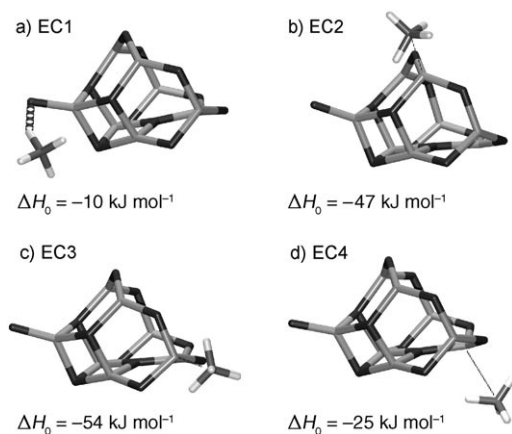


Figure 5. Four different encounter complexes (EC): a) Reactive EC1 formed in the reaction $\text{Al}_8\text{O}_{12}^{+} + \text{CH}_4 \rightarrow \text{Al}_8\text{O}_{11}(\text{OH})^{+} + \text{CH}_3^{\bullet}$ with methane; b) EC2, c) EC3, and d) EC4 are formed by coordination of methane to the Lewis acidic, threefold-coordinated aluminum atoms in the cluster.

H–O bond length is 197 pm, whereas the C–H bond is slightly elongated and the Al–O bond slightly shortened (Figure 4). Frequency calculations of the encounter complex show that it corresponds to a genuine minimum on the PES. The reaction proceeds then by a transition structure (TS) that is characterized by the transfer of the interacting hydrogen atom to the radicaloid oxygen atom.^[19] Without considering the zero-point energy (ZPE), the energy of the TS is minimally higher (by ca. 0.2 kJ mol^{-1}) than that of the encounter complex. Taking the ZPE into account the barrier vanishes, and the energy of the TS is 4 kJ mol^{-1} below the encounter complex.

Whether or not a local minimum exists, and how much lower the TS is than the entrance channel, depends crucially on the accuracy of the B3LYP/TZVP method used. Coupled-cluster calculations with inclusion of triple substitutions and with extrapolation to the complete basis set, CCSD(T), for the prototype reaction of MgO^{+} with methane (see Supporting Information) show that, compared to the

B3LYP/TZVP calculations employed herein, the encounter complex is stabilized by $13\text{--}15 \text{ kJ mol}^{-1}$, whereas the transition structure is destabilized by only 2.5 kJ mol^{-1} . This means that B3LYP/TZVP underestimates the stability of the encounter complex (most likely because of missing dispersion interactions) and it also underestimates the intrinsic energy barrier, TS–EC, by 23 kJ mol^{-1} . The latter value fits into the general performance of B3LYP, for which a mean signed error of -17 kJ mol^{-1} has been reported for energy barriers of 38 hydrogen transfer reactions.^[20]

Figure 4 depicts the structural details of the hydrogen-atom transfer. The primary reaction product contains a hydroxy group that still interacts with the methyl radical formed; however, the interaction is quite small, as also indicated by their rather long distance, and the interaction energy amounts to only 8 kJ mol^{-1} . The formation of the primary product is quite exothermic ($\Delta_r H_0 = -99 \text{ kJ mol}^{-1}$) and the overall energy liberated in the production of separate fragments ($\text{Al}_8\text{O}_{11}(\text{OH})^{+} + \text{CH}_3^{\bullet}$) equals -91 kJ mol^{-1} .

As $\text{Al}_8\text{O}_{12}^{+}$ has three symmetry-inequivalent, threefold coordinated aluminum atoms (overall five: two symmetry-equivalent pairs exist), which are expected to be strongly Lewis acidic, and thus additional encounter complexes are predicted to exist.^[16] This is borne out by the computations: Four isomeric encounter complexes were located on the PES (Figure 5). EC1 corresponds to the reactive complex discussed above (Figure 4), and is thermodynamically the least stable of the four structures. The other complexes exhibit stronger association energies, ranging from -25 to -54 kJ mol^{-1} . Their magnitudes appear too large to be attributed solely to electrostatic interactions, but taking into account the formally triple charge of the predominantly interacting aluminum atoms, it is a reasonable value for an ion-induced dipole complex. In EC4 the unperturbed aluminum atom is coordinated in a planar threefold fashion that has to be distorted for the interaction with methane. In EC2 and EC3 the reacting aluminum atom occupies a distorted threefold coordination, which is almost a tetrahedron with a missing vertex. The carbon atom in methane is found at this empty vertex, acting as a Lewis base. The Al–C distances are in the range of 235 to 254 pm, thus reflecting rather weak interactions. Finally, as a result of the complexation the H–C–H angles of the organic molecule are also distorted.

As the reactive encounter complex is energetically disfavored in comparison to the three other complexes, it might be expected that a molecular adduct $\text{Al}_8\text{O}_{12}(\text{CH}_4)^{+}$ would be observed as the main product of the reaction, which is not observed experimentally. However, the reaction conditions need to be taken into account. As the IMR occurs under conditions of strictly bimolecular collision ($T = 298 \text{ K}$; $p(\text{CH}_4) = 9 \times 10^{-8} \text{ mbar}$), the encounter complex can be stabilized only by infrared emission.^[21] This process becomes efficient only in larger systems or with significantly higher interaction energies. Thus, the encounter complexes EC2–EC4 form, but are short-lived and dissociate back to the reactants. Only if CH_4 hits the cluster surface in the vicinity of the oxygen centered radical, the barrierless hydrogen abstraction occurs and the product complex can dissociate, releasing the methyl radical. Thus, the generation of short-lived

encounter complexes is a necessary consequence of the not-negligible geometric size of the cluster, and accounts for the low rate constant of reaction (2).^[22]

The present combined experimental and theoretical study provides the first example for the thermal activation of methane by a polynuclear main-group metal oxide cluster. This observation is quite significant, as the often extremely reactive mononuclear metal oxides should not be considered as ideal model systems relevant for an understanding of a real-life oxidation catalyst; as stated earlier, the investigations of larger systems, that is, cluster metal oxides, are more appropriate to serve this purpose.^[10,23,24]

Experimental Section

The experiments are carried out using a Bruker/Spectrospin CMS47X FT-ICR mass spectrometer equipped with an external laser vaporization source and an APEX III data station.^[25,26] Aluminum oxide clusters are generated by laser ablation of an aluminum target, followed by cooling of the hot aluminum plasma by the expanding helium gas (15 bar) that contains about 2% molecular oxygen. Clustering takes place while traveling through a metal tube. A series of potentials and ion lenses is used to transfer the ions to the ICR cell, which is positioned in the bore of a superconducting magnet (4.5 T). Finally, cluster distributions of Al_nO_m^+ are observed with $n = 3-5$ and $m = 5-15$, depending on the content of oxygen and duration of cell opening. Reactions of the mass-selected aluminum oxide cluster cations Al_nO_m^+ of interest are then studied by introducing methane by a leak valve at stationary pressures (9×10^{-8} mbar).

Calculations are performed using B3LYP^[27] with triple- ζ -plus-polarization basis sets (TZVP)^[28] employing Turbomole 5.9.^[29] Zero-point energy (ZPE) corrections are calculated in the harmonic approximation based on analytical derivatives of the energy with respect to the nuclear coordinates.^[30,31]

Received: October 16, 2007

Revised: November 11, 2007

Published online: January 28, 2008

Keywords: aluminum oxide · C–H activation · density functional calculations · mass spectrometry · methane

- [1] D. R. Stull, E. F. Westrum, Jr., G. C. Sinke, *The Chemical Thermodynamics of Organic Compounds*, Wiley, New York, **1969**, p. 865.
- [2] J. Berkowitz, G. B. Ellison, D. Gutman, *J. Phys. Chem. B* **1994**, *98*, 2744.
- [3] a) D. H. R. Barton, *Aldrichimica Acta* **1990**, *23*, 3; b) B. A. Arndtsen, R. G. Bergman, T. A. Mobley, T. H. Peterson, *Acc. Chem. Res.* **1995**, *28*, 154; c) G. A. Olah, A. Molnár, *Hydrocarbon Chemistry*, Wiley, New York, **1995**.
- [4] A. A. Fokin, P. R. Schreiner, *Chem. Rev.* **2002**, *102*, 1551.
- [5] a) S. T. Ceyer, *Science* **1990**, *249*, 133; b) Z. Zhang, X. E. Verykios, M. Baerns, *Catal. Rev. Sci. Eng.* **1994**, *36*, 507; c) X. Bao, M. Muhler, R. Schlögl, G. Ertl, *Catal. Lett.* **1995**, *32*, 185; d) A. J. Nagy, G. Mestl, R. Schlögl, *J. Catal.* **1999**, *188*, 58.
- [6] a) D. Schröder, A. Fiedler, J. Hrušák, H. Schwarz, *J. Am. Chem. Soc.* **1992**, *114*, 1215; b) D. Schröder, H. Schwarz, S. Shaik, *Structure and Bonding* (Ed.: B. Meunier), Springer, Berlin, **2000**, p. 97.
- [7] I. Kretzschmar, A. Fiedler, J. N. Harvey, D. Schröder, H. Schwarz, *J. Phys. Chem. A* **1997**, *101*, 6252.
- [8] M. K. Beyer, C. B. Berg, V. E. Bondybey, *Phys. Chem. Chem. Phys.* **2001**, *3*, 1840.
- [9] K. K. Irikura, J. L. Beauchamp, *J. Am. Chem. Soc.* **1989**, *111*, 75.
- [10] S. Feyel, J. Döbler, D. Schröder, J. Sauer, H. Schwarz, *Angew. Chem.* **2006**, *118*, 4797; *Angew. Chem. Int. Ed.* **2006**, *45*, 4681.
- [11] D. Schröder, J. Roithová, *Angew. Chem.* **2006**, *118*, 5835; *Angew. Chem. Int. Ed.* **2006**, *45*, 5705.
- [12] Except for FeO^+ : Here, the bonding blocks contain one filled σ orbital, two filled π orbitals, and two singly occupied π^* orbitals, resulting in high-spin situations. For further information, see: S. Shaik, M. Filatov, D. Schröder, H. Schwarz, *Chem. Eur. J.* **1998**, *4*, 193.
- [13] J. Sauer, *Computational Modeling of Principles and Mechanisms of Transition Metal-Based Catalytic Processes* (Eds.: K. Morokuma, J. Musaev), Wiley-VCH, Weinheim/New York, in press.
- [14] The spin densities for MgO^+ , $\text{V}_4\text{O}_{10}^{4+}$, and $\text{Al}_8\text{O}_{12}^{4+}$ are almost exclusively localized at one of the terminal oxygen atoms; for MoO_3^+ , the spin is only slightly delocalized, and OsO_4^+ and $\text{ReO}_3(\text{OH})^+$ show delocalization among two oxygen atoms. FeO^+ corresponds to a high-valent diradicaloid cation exhibiting also a high spin density at the oxygen atom; see also references [6] and [12].
- [15] This view is also supported by a computational study of the closed-shell system CaO/CH_4 . While H-atom abstraction is slightly exothermic, the barrier of the process is huge: H.-Q. Yang, C. W. Hu, S. Qin, *Chem. Phys.* **2006**, *330*, 343.
- [16] M. Sierka, J. Döbler, J. Sauer, G. Santambrogio, M. Brümmer, L. Wöste, E. Janssens, G. Meijer, K. Asmis, *Angew. Chem.* **2007**, *119*, 3437; *Angew. Chem. Int. Ed.* **2007**, *46*, 3372.
- [17] The atomization energy of $1/2 \text{ H}_2$ needs to be added to obtain the C–H binding energy in methane.
- [18] In Figure 2a, it cannot be distinguished between H-abstraction from CH_4 or any other impurity in the cell. Although Figure 2b shows adduct formation with water, the conceivable uptake of a hydrogen atom from water to form $\text{Al}_3\text{O}_7(\text{OH})^+$ can be rejected on thermochemical grounds and experimental evidence. Furthermore, the rate constant of the hydrogen addition is so small that any impurity present at an absolute pressure of 1.0×10^{-10} mbar which reacts with collision rate may be the origin of the $\Delta m = +1$ product.
- [19] The structure is a true saddle point on the PES: the gradients are zero, and frequency calculation yields one imaginary frequency with a corresponding mode that consists mainly of motion of the interacting hydrogen atom.
- [20] Y. Zhao, D. G. Truhlar, *J. Phys. Chem. A* **2005**, *109*, 5656.
- [21] a) R. C. Dunbar, *Mass Spectrom. Rev.* **1992**, *11*, 309; b) R. C. Dunbar, S. J. Klippenstein, J. Hrušák, D. Stöckigt, H. Schwarz, *J. Am. Chem. Soc.* **1996**, *118*, 5277.
- [22] Note that CD_4 is not orbiting the cluster before the collision. Previously it has been shown that the Langevin capture cross-section is smaller than the physical dimensions of the cluster for a large fraction of the neutral collision partners. Only a very small fraction of neutral molecules is actually captured by the charge; the vast majority undergo direct impact on the cluster surface. See: G. Kummerlöwe, M. K. Beyer, *Int. J. Mass Spectrom.* **2005**, *244*, 84.
- [23] A. Fielicke, K. Rademann, *J. Phys. Chem. A* **2000**, *104*, 6979.
- [24] V. B. Goncharov, *Kinet. Catal.* **2003**, *44*, 499.
- [25] Laser Vaporization: a) V. E. Bondybey, J. H. English, *J. Chem. Phys.* **1981**, *74*, 6978; b) T. G. Dietz, M. A. Duncan, D. E. Powers, R. E. Smalley, *J. Chem. Phys.* **1981**, *74*, 6511; c) S. Maruyama, L. R. Anderson, R. E. Smalley, *Rev. Sci. Instrum.* **1990**, *61*, 3686; d) K. R. Asmis, J. Sauer, *Mass Spectrom. Rev.* **2007**, *26*, 542.
- [26] ICR and ion/molecule reactions: a) C. Berg, T. Schindler, G. Niedner-Schatteburg, V. E. Bondybey, *J. Chem. Phys.* **1995**, *102*, 4870; b) I. Balteau, O. P. Balaj, M. K. Beyer, V. E. Bondybey,

- Phys. Chem. Chem. Phys.* **2004**, 6, 2910; c) K. Eller, H. Schwarz, *Int. J. Mass Spectrom. Ion Processes* **1989**, 93, 243.
- [27] a) C. Lee, W. Yang, R. G. Parr, *Phys. Rev. B* **1988**, 37, 785; b) A. D. Becke, *J. Chem. Phys.* **1993**, 98, 5648.
- [28] A. Schäfer, C. Huber, R. Ahlrichs, *J. Chem. Phys.* **1994**, 100, 5829.
- [29] a) R. Ahlrichs, M. Bär, M. Häser, H. Horn, C. Kölmel, *Chem. Phys. Lett.* **1989**, 162, 165; b) O. Treutler, R. Ahlrichs, *J. Chem. Phys.* **1995**, 102, 346; c) K. Eichhorn, F. Weigand, O. Treutler, R. Ahlrichs, *Theor. Chem. Acc.* **1997**, 97, 119; d) M. von Arnim, R. Ahlrichs, *J. Chem. Phys.* **1999**, 111, 9183.
- [30] a) P. Deglmann, F. Furche, R. Ahlrichs, *Chem. Phys. Lett.* **2002**, 362, 511; b) P. Deglmann, F. Furche, *J. Chem. Phys.* **2002**, 117, 9535.
- [31] Note added in proof (January 16, 2008): In a recent publication, odd/even electron alternations were reported for the gas-phase reactions of oxygen with aluminum-based cluster ions: A. C. Reber, S. N. Khanna, P. J. Roach, W. H. Woodward, A. W. Castleman, Jr., *J. Am. Chem. Soc.* **2007**, 129, 16098.
-